OBIA-based Monitoring of Riparian Vegetation Applied to the Identification of Degraded Acacia Xanthophloea along Lake Nakuru, Kenya

Anne Osio, Sébastien Lefèvre, Patrick Ogao, Samson Ayugi

HAL Id: hal-01960341

https://hal.univ-reunion.fr/hal-01960341v1

Submitted on 13 Feb 2019

OBIA-based Monitoring of Riparian Vegetation Applied to the Identification of Degraded Acacia Xanthophloea along Lake Nakuru, Kenya.

Anne Osio [1], Sébastien Lefèvre [2], Patrick Ogao [1], Samson Ayugi [1]

1. Technical University of Kenya
Haile Selassie Avenue, PO Box 52428, 00200 Nairobi, Kenya
{ansiyo22@gmail.com, ogaopj@gmail.com, okothayugi@gmail.com}

2. Univ. Bretagne Sud, IRISA UMR 6074
Campus de Tohannic, 56017 Vannes, France
sebastien.lefevre@irisa.fr

ABSTRACT. The Lake Nakuru (Kenya) faces flooding since 2010, thus interfering with the growth of riparian vegetation, and requiring automated image analysis to monitor the effect of flooding on the Lake Nakuru Riparian Reserve vegetation species. The vegetation specie that was affected by the flooding lake is Acacia Xanthophloea, i.e. a habitat and feed for many animal species within the National Park. In this study, we explore how *an OBIA methodology can provide* riparian vegetation classification*, thus eas*ing the detection of degraded Acacia Xanthophloea spp. Our study shows that: i) from a thematic point of view, GEOBIA was able to identify Acacia Xanthophloea from Landsat satellite imagery, and comparing the resulting classification maps allows us to achieve monitoring of this specie through time; ii) from a software point of view, it might be necessary to involve several different tools (both proprietary or open source) since there is still some missing functionalities in the existing GEOBIA software solutions.
KEYWORDS: Remote sensing, OBIA, Change detection, Vegetation Monitoring, Landsat Imageries, Thematic classification.

1. Introduction

Object-based image analysis has been used in various change detection studies (Lunneta *et al.,* 2006; Ma *et al.,* 2016). Object-oriented classification describes relationships in terms of several categories of characteristics each of which being assigned certain weightings. Object features include properties such as color, texture, shape, area and scale. Previous studies have also shown that the common pixel-based approach used in remote sensing imagery classification has drawbacks, in that it causes noise in the output image, otherwise known as the 'salt and pepper' effect (Oke *et al.,* 2012). The OBIA approach to image classification has been used on land use and riparian studies (Dupuy *et al.,* 2012; Tormos *et al.,* 2012). The method has been applied over wide areas covered by High and Very High Spatial Resolution satellite imageries. It provides an effective computer-assisted classification technique whose results are close to the manual photo-interpretation. According to research carried out by Durieux *et al.* (2007) and Tiede *et al.* (2010), this method is faster, cheaper and more reproducible than pixel-based approach.

The basis of OBIA is the traditional segmentation method, where pixels containing the object to be studied are measured against the spatial extent of the object. The underlying principle of the system uses a region growing technique, which starts with regions of one pixel in size based on the spectral and spatial characteristic of the pixels under study (Baatz *et al.,* 2004). The local homogeneity criteria are then used to make decisions about merging regions of interest by taking into account the image analyst's expertise. The goal of multiscale segmentation is to build a hierarchical set of image object primitives at different resolutions by appending multi-resolution segmentation maps in which objects are subject of coarse structures. The parameters controlling the algorithm include scale, homogeneity criteria, shape and color. Object-based image analysis (OBIA) allows for use of variables such as texture, shape, context and other cognitive information provided by the image analyst to segment and classify image features thus improving classification.

OBIA method of classification improves the accuracy results and allows mapping of very small urban features, such as mature individual trees or small clusters of shrubs (Platt and Rapoza, 2008; Hay *et al.,* 2005). Other studies have shown that pixel-based classification approaches, although appropriate on Landsat Imagery, are outperformed by OBIA approaches on hyper spectral images in urban, sub-urban and agricultural landscapes (Platt and Rapoza, 2008) and in urban-wildland interface, especially in instances where tree cover is complex and heterogeneous (Tuominen and Pekkarinen, 2005). OBIA algorithm is capable of extracting the indices of various land cover features. Satellite imagery of high or very high spatial resolution has been used in various studies to extract indices assuming presence of channels with Top of the Atmosphere (TOA) reflectance. The first step involves conversion of raw data into TOA spectral radiance, then converting the spectral radiance into spectral reflectance. TOA bands include Red, Green and Near-Infra-Red (NIR) bands. The feature view tool in eCognition enables calculation of Vegetation, Water and Soil index. According to McFeeters (1996), vegetation indices range between 0 and 1. Normalized Difference Vegetation Index (NDVI) closer to 1 indicates healthy vegetation while

negative NDVI indicates stressed vegetation. Measuring of NDVI is made possible through thresholding in eCognition (Ma *et al.,* 2016). The threshold map is then exported to ArcGIS 10 for thematic re-classification (Sakamoto *et al.,* 2007). There is dire need on the improvement of classification methods using the recently developed classification algorithms and classifiers such as random forests, J48 decision tree, CART and Naïve Bayes in order to achieve a better classification model. Accuracy of classification being a method of classification stability has been applied in recent research studies. Accuracy assessment carried out on OBIA is known to be high (>85%) compared to non-OBIA approaches. It compares how each element (e.g., pixel- is classified against the definite land cover condition obtained from the corresponding ground truth data. *Specificity* and *Sensitivity* are two aspects in accuracy assessment where results are determined by the classification of specific terrain classes of the predicted elements against the observed ones. The *sensitivity* of the model is the proportion of positive pixels correctly predicted (*i.e.,* the probability that a pixel belonging to a particular category is correctly identified). The *specificity* of the model is the proportion of negative pixels correctly predicted (*i.e.,* the probability that a pixel not belonging to a particular category is correctly identified). Thus, models with high sensitivity can correctly predict positive pixels (pixels belonging to the category of interest) and models with high specificity can correctly predict negative pixels (pixels not belonging to the category of interest). High sensitivity is usually associated with poor specificity, which manifests as an overestimate of area in the category of interest. An optimum classification model would be one with the highest possible value of sensitivity and specificity, minimizing omission and commission errors at the same time. Since this ideal situation is usually not the case, there is a need to make a compromise, and the ROC curve is an appropriate tool to make such a choice.

2. Materials and Methods

In this section, we successively present the data capture, preprocessing, processing, and analysis.

2.1. Data Capture

Raw satellite data were downloaded from the USGS site. The study area fell specifically within path 169 and row 060.The datasets were of the same datum and projection, *i.e.,* WGS 84/UTM Zone 36N. Datasets were as follows: Landsat 5 TM collected on 17.01.2011, Landsat 8 OLI dated 2014, and Landsat 8 OLI dated 16.12.2016.

2.2 Data Pre-processing

Preprocessing of datasets was carried out on the imageries in order to remove noise and enable uniformity between datasets. Band compositing was carried out followed by subsetting of the four imageries, using Erdas Imagine. Each image was pan-

sharpened to 15m resolution using Ehlers fusion technique. The panchromatic bands that came with each dataset have been used in each case. The final products were Landsat imageries of false colours with band combination RGB (4, 3, 2).

In order to convert raw values (DN) to Top of the Atmosphere (TOA) reflectance, the images were uploaded in ArcGIS 10.4 whereby procedures were carried out using the spatial analyst tool in ArcToolbox using the following equation:

$$\rho\lambda = M_\rho\, Q_{cal} \,+\, A_\rho \tag{1}$$

with $\rho\lambda$ the TOA planetary reflectance, without correction for solar angle (NB does not contain a correction for sun angle), M_ρ and A_ρ the band-specific multiplicative rescaling factor and additive rescaling factor from metadata (Reflective_Add_Band_X, where X is the band number), and Q_{cal} the quantized and calibrated standard product pixel values (DN). In case a correction for the sun angle is needed, the computation becomes

$$\rho\lambda = \frac{\rho\lambda'}{\cos(\theta_{SZ})} = \frac{\rho\lambda'}{\sin(\theta_{SE})} \tag{2}$$

with θ_{SE} the local sun elevation angle and θ_{SZ} the local solar zenith angle ($\theta_{SZ} = 90 - \theta_{SE}$). The scene center sun elevation angle in degrees is also provided in the metadata (Sun_Elevation).

The three Landsat Images were then cropped to the shape of the study area in ArcGIS in readiness for export into eCognition Developer. The scene size was (936 x 1520) pixels in spatial extent.

2.3. Data Processing

The images were then uploaded into eCognition Developer of which the first step was to convert the pixels into image objects by the use of multiresolution segmentation algorithm. The layer weights adopted on the 2011 Landsat 5 TM image prior to classification were scale = 5, shape = 0.2, and compactness = 0.7. The Green, Red, NIR and SWIR bands were useful in the calculation of vegetation indices on each dataset. A variety of the indices were calculated and captured in eCognition database link tables which could only be viewed when exported to ArcGIS interface. The values that were captured through the customized tool in eCognition were mean Red, Green, NIR, SWIR1 and SWIR2. Rulesets were thus formed in the feature view section so as to come forth with NDVI values which were calculated from eCognition customized tool. Supervised classification by sample selection was carried out on each image using the k-NN Algorithm. Initially, from the 2011 imagery it was possible to extract vegetation classes using the previous studies by Mutangah (1994). Using a sample selection method, the following classes of vegetation were thus created: Acacia Xanthophloea, Chloris Gayana grasslands, Bushed Themada Triandra grasslands, Cynodon Niemfluensis grasslands, Cynodon Niemfluensis wooded Acacia Xanthophloea grasslands, Cynodon Chloris Themada grasslands, Lake Nakuru, Sedges & Marshes, Sand & Mud flats, Sporobolus Spicatus grasslands, Tachonandus bush land, Euphorbia candelabra and the highland vegetation.

2.4. Data Analysis

Several aspects were observed in this study, namely: i) the classification scales used on each image; ii) pan-sharpening methods and type of sensors used; iii) type of classification used (thresholding or sampling); iv) procedures used in atmospheric, radiometric, and geometric corrections; v) classification algorithms and modes used.

Classification scales varied across the different images, thus giving rise to different number of instances per imagery. These instances were then used to measure the significance of the number of instances on classification accuracy. Pan-sharpening methods used on the imagery were Ehlers fusion and IHS. Type of classification in eCognition Defiens can either be through sampling or thresholding using the feature view tool. In this study the sample selection technique was used. Procedures used in atmospheric corrections involve the conversion of raw DN values to at sensor reflectance. Using the MTL files that come in handy with the downloaded images, values can be inserted into equations (1) and (2) to come up with TOA reflectance imageries. The main goal is to be able to calculate vegetation indices from the same images. NDVI values were calculated in eCognition and NDVI maps were also generated from ArcGIS 10.4. Other vegetation indices were also included in the rule sets, *i.e.*, Green Normalized Difference Vegetation Index. Finally, the CSV files and the shape files of the imageries were exported to ArcGIS for further editing and processing and transited to Weka software for further analysis.

The classifier that was used on the datasets in eCognition was k-NN algorithm, while the ones used in Weka were J48, Random Forest, Binary Support Vector (SMO) and Naïve Bayes. We looked at the classifier performance on each dataset which was initially generated in eCognition. The classification modes explored were full training, data split in 2/3 for training and 1/3 for testing, and 10-fold cross-validation. OBIA supervised classification was appended on the different datasets from different dates in order to find out the best classification models. It was worth investigating the effect of classification scales and sample size on classification accuracy.

3. Results and Discussion

3.1. The study area

Lake Nakuru National Park is located geographically at $36°$ 03' 00'' East of Latitude and $00°$ 14' 24'' South of Longitude. It is located 170kms from Nairobi to Nakuru, along the Trans African Highway. On the Eastern part of the lake lays the Euphorbia species of vegetation, just on the lion hill range. The western part of the lake is covered by cliffs (baboon cliff) and rock outcrops. The total study area is 188km^2 (Mwasi, 2002) with average rainfall ranging between 876mm and 1050mm. Mean daily minimum and maximum temperatures are $8.2°$C and $25.6°$C. Lake Nakuru lies on the floor of the Kenyan Rift Valley with an approximate altitude range of 1760-2080m above sea level. The study area (Figure 1) falls under Agro-Ecological Zone (AEZ) Upper Midland 5 (UM5) also known as the Livestock-Sorghum Zone.

According to 1982 soil surveys, the soils are sodic, while the texture is medium to heavy (m-h).
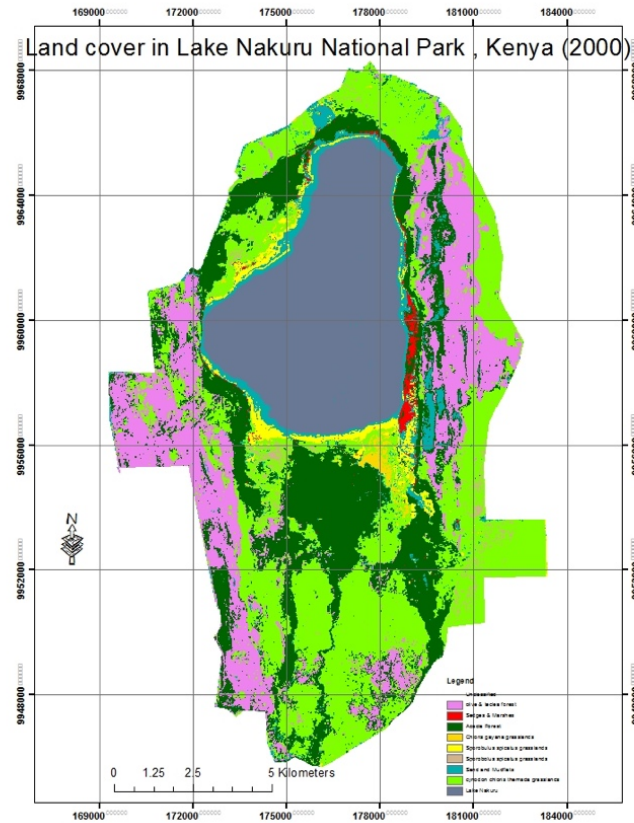

FIGURE *1. Baseline map of the study area*

3.2. Supervised Classification on baseline imagery

After defining the training classes, supervised classification by non-parametric rule is appended on the image, illustrated by one or more training areas. The entire signature rows and columns have to be selected in order to be used in the classification process. The image was then classified into nine classes: Olive & Teclea forest, Lake Nakuru, Sedges & Marshes, Chloris Gayana grasslands, Acacia forest, Sporobolus Spicatus grasslands, Cynodon Chloris Themada grasslands, Sand & Mudflats, Escarpment vegetation, Euphorbia Candelabra and Tachonandus bush land. AOI's was thus enhanced to produce spectral signatures belonging to each given class. Signature (SIG) file were created from the signature editor table in Erdas Imagine

2014. The signatures were saved in folders which could be retrieved and appended on the other images for image analysis.

3.3. Object based classification

3.1.1. Segmentation parameters

The process used in segmenting the images into objects was multiresolution segmentation algorithm in eCognition Developer 9.2. Major features that were incorporated into the image segmentation routine when setting segmentation parameters were:

- *Layer weights*: there are layers with more important information about particular features for segmentation process; they are thus given higher weight.

- *Scale parameters* that measures the maximum change of heterogeneity when merging image objects.

- *Composition of homogeneity criterion* that prioritizes the drivers for object creation such as "colour has preference to shape".

The outlined parameters were set in eCognition Developer 9.2 which used multiresolution segmentation (Table 1) which divides the image into homogenous image objects based on how close the value of the neighboring pixel in relation to the class under study. In eCognition developer 9.2, the band mixing tool was used in generating false positive image with RGB { 5, 4, 3 } band combination for Landsat 8 OLI 2014 (*i.e.*, NIR, R, G) while RGB { 4, 3, 2 } for Landsat 5 TM 2011 and Landsat 8 OLI 2016 (*i.e.*, NIR, R, G). The following segmentation scales were then set as shown in the aforementioned table.

TABLE *1. Segmentation scales appended in eCognition Defiens*

Image	scale	shape	compactness	Red	Blue	Green	NIR
Landsat5TM_2011	5	0.2	0.7	1	1	1	1
Landsat8OLI_2014	40	0.5	0.5	1	1	1	1
Landsat8OLI_2016	20	0.2	0.7	1	1	1	1

3.1.2. Appending of rulesets in eCognition

Rulesets were developed within the eCognition feature view. This involved the calculations which were made possible through the use of the customized toolbar. The ruleset (Figure 2) includes NDVI which was used to measure vegetation vitality. Per pixel area was also important in measuring the spectral information of vegetation species within Lake Nakuru National Park. Figure 2 depicts the type of indices that were appended on Landsat5TM_2011 Imagery.
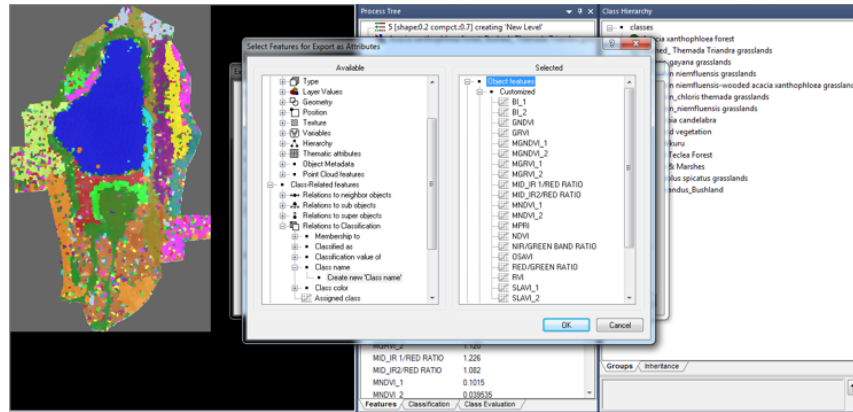
FIGURE *2. Appending of rulesets in eCognition*

3.4. Accuracy assessment on the datasets

The link tables associated with the classification (CSV files) and the shapefile of the mapped image was exported to ArcGIS 10.4 for thematic re-classification which is a process that entails editing of datasets. It was observed that the re-classification was only possible through the use of iso-data classifier in ArcGis. Thematic reclassification was done in order to add sub-vegetation species such as Acacia Xanthophloea re-growth (Acacia Saplings). The process of object-based supervised classification on each image was then carried in Weka software. This process led to poor classification results on Landsat 8 OLI 2014 except for the Random Forest classifier which recorded a kappa coefficient of 1.0 and J48 with a kappa value of 0.72. Landsat 5 TM 2011 and Landsat 8 OLI 2016 did not undergo thematic re-classification which is why excellect classification results were realized such as on Landsat 5 TM 2011 where Random Forest and J48 had the highest kappa statistic of 1.0. Landsat 8 OLI 2016 realized a kappa value of 1.0 from Random Forest and of 0.92 from J48. For the sake of illustration, confusion matrices obtained for classification with Random Forest on the 3 images are provided in Tables 2-4.

TABLE 2: *Confusion Matrix, Random Forest classification on Landsat 5 TM 2011. FID: (a) Lake Nakuru, (b) Acacia Xanthophloea, (c) Euphorbia Candelabra, (d) Cynodon Chloris Themada grassland, (e) Chloris Gayana grasslands, (f) Bushed Themada Triandra grassland, (g) Tachonandus bushland, (h) Sedges & Marshes, (i) Cynodon Niemfluensis grasslands, (j) Cynodon Niemfluensis wooded acacia grasslands, (k) Sporobolus Spicatus grasslands, (l) Cynodon grasslands, (m) Olive & Teclea forest, (n) Highland vegetation*

FID	a	b	c	d	E	f	g	h	i	j	k	l	m	n	Total
a	860														860
b		891													891
c			311												311
d				264											264
e					172										172
f						88									88
g							211								211
h								87							87
i									203						203
j										396					396
k											202				415
l												394			230
m													415		415
n														230	230
Total	860	891	311	264	172	88	211	87	203	396	415	230	415	230	4724

TABLE 3: *Confusion Matrix, Random Forest classification on Landsat 8 OLI 2014. FID: (a) Acacia forest, (b) Acacia saplings, (c) Acacia savannah, (d) Acacia woodlands, (e) Chloris Gayana grasslands, (f) Cynodon Chloris Themada grasslands, (g) Cynodon Niemfluensis grasslands, (h) Highland Vegetation, (i) Euphorbia Candelabra, (j) Lake Nakuru, (k) Sand & Mudflats, (l) Sedges & Marshes, (m) Sewerage plant, (n) Tachonandus bushland*

FID	a	b	c	d	e	f	g	h	i	j	k	l	m	n	Total
a	119														119
b		421													421
c			431												431
d				154											154
e					190										190
f						10									10
g							70								70
h								45							45
i									30						30
j										25					25
k											108				108
l												10			10
m													4		4
n														1	1
Total	119	421	431	154	190	10	70	45	30	25	108	10	4	1	1618

TABLE 4: *Confusion Matrix, Random Forest classification on Landsat 8 TM 2016. FID: (a) Cynodon Niemfluensis grasslands, (b) Sporobolus Spicatus grasslands, (c) Lake Nakuru, (d) Acacia Xanthophloea, (e) Euphorbia Candelabra, (f) Cynodon Niemfluensis wooded Acacia grasslands, (g) Tachonandus bushland, (h) Chloris Gayana, (i) Olive & Teclea forest, (j) Highland vegetation, (k) Cynodon Chloris Themada grasslands, (l) Bushed Themada Triandra grasslands*

FID	a	b	c	d	e	f	g	h	i	j	k	l	Total
a	2717												2717
b		121											121
c			1024										1024
d				465									465
e					280								280
f						175							175
g							193						193
h								128					128
i									122				122
j										149			149
k											157		157
l												10	10
Total	2717	121	1024	465	280	175	193	128	122	149	157	10	5541

3.5. Change detection on land cover

The main vegetation specie under investigation was Acacia Xanthophloea. Spatial change detection was possible through observing the per pixel area of the vegetation under study. The Lake Nakuru area was observed to have increased from 860 pixels in 2011 to 1024 pixels in 2016, thus confirming reports by Onywere *et al.* (2013) that the lake has been flooding its banks. The area covered by Acacia Xanthophloea was 891 pixels in 2011 but reduced to 465 pixels in 2016. Thus, the difference in spatial coverage (426 pixels) of Acacia Xanthophloea was covered by the flooded lake. Other vegetation species closer to the lakes which were affected by the flooding were sedges and marshes whose area was 87 pixels and Cynodon Chloris Themada grasslands with area of 264 pixels, both on Landsat 5 TM 2011. They were not detected on the Landsat 8 OLI 2016. Cynodon Niemfluensis grasslands seem to have thrived in the flooded plain and thus an increase in their spatial coverage from 597 pixels in 2011 to 2317 pixels in 2016. Other vegetation species with area reduced under the study period are as follows: Chloris Gayana (44 pixels), Bushed Themanda Triandra (78 pixels), Tachonandus Bush land (18 pixels), Sporobolus Spicatus grasslands (81 pixels), highland vegetation (73 pixels) and Olive & Teclea forest (266 pixels).

3.6 Spectral characteristics of vegetation

Spectral characteristics were observed on the classified baseline image *i.e.*, Landsat 5 TM 2010 (Figure 3). Sand & Mudfats reflected more seconded by Chloris Gayana. The lowest reflectance was depicted by the Lake Nakuru whose graph indicated that the waters were clear. From the NDVI maps (Figure 4) generated from Landsat 5 TM

2011 ranged from -0.19 to +0.63, Landsat 8 OLI 2014 ranged from -0.062 to +0.24 while on Landsat 8 OLI 2016 the range was from -0.19 to +0.16. These results thus confirm reports that the Lake Nakuru National Park ecosystem has been degrading.
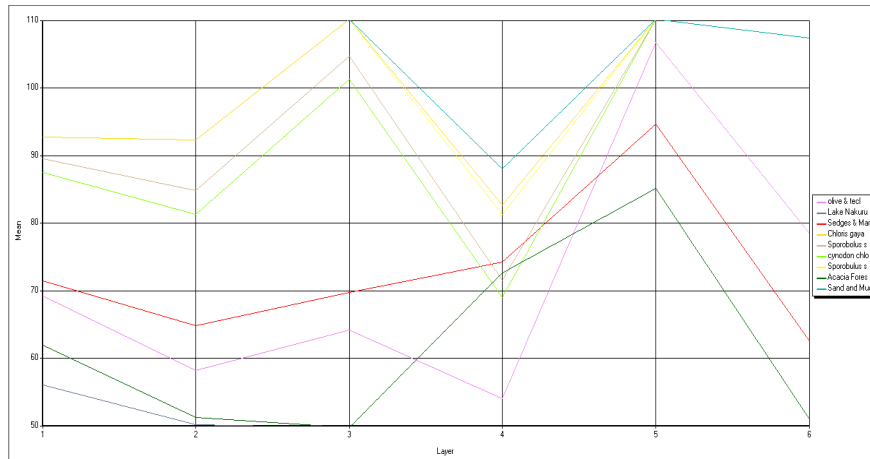

FIGURE *3. Spectral signatures of land cover classes in Lake Nakuru National Park*
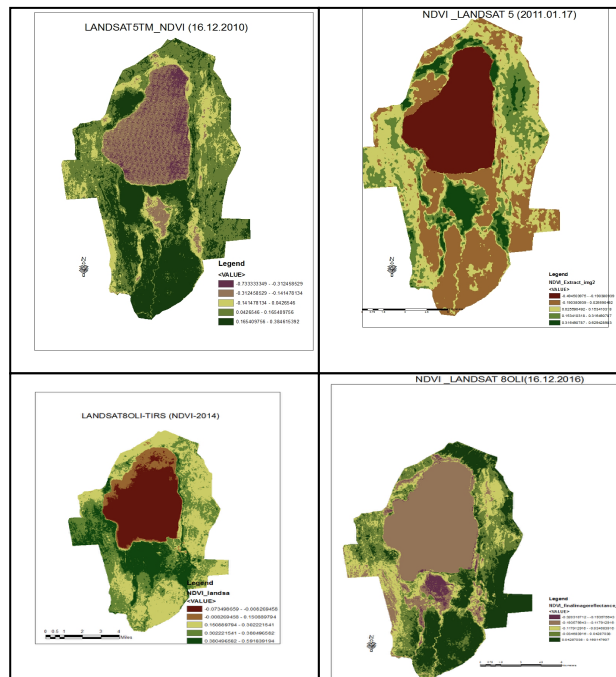

FIGURE 4. NDVI Maps (2010-2016)

4. Conclusion

The spatial and spectral changes that were detected in this study indicate the degradation of a variety of vegetation species in the National Park. Since the study focuses on Acacia Xanthophloea, further studies will be carried out on individual acacia trees which have been immersed in water. This will be made possible by the use of template matching algorithm in eCognition. It was also noted that accuracy of supervised object-based classification in Weka depends on the size of the datasets uploaded into its environment. Accuracy assessment (Coagalton and Green, 1999) on different datasets in Weka software revealed that J48 classifier had an overall accuracy of 0.72 while Random Forest classifier achieves an overall accuracy of 1.0 on Landsat 8 OLI 2014. Accuracy assessment on Landsat 5 TM 2011 revealed that both Random Forest and J48 classifiers had an overall accuracy of 1.0. On Landsat 8 OLI 2016, overall accuracy by J48 classifier was 0.92 and 1.0 by Random Forest classifier. Comparing the areas covered by healthy acacia using year 2011 imagery as a baseline, it was noted that in 2011 the area covered with Acacia Xanthophloea was 891 pixels which was noted to have reduced to 465 pixels by the year 2016. This confirms reports by Onywere *et al.* (2013) that indeed the lake's riparian has been flooding. Another observation made from this practical study is the need of various software to conduct the GEOBIA-based analysis. It is thus calling for a unified, open-source solution.

References

Baatz, M., Benz, U., Dehghani, S., Heynen, M., Höltje, A., Hofmann, P., Lingenfelder, I., Mimler, M., Sohlbach, M., Weber, M., et al., 2004. eCognition Professional User Guide; Definiens Imaging GmbH: München.

Congalton, R.G. and K. Green, 1999. Assessing the Accuracy of Remotely Sensed Data: Principles and Practices. Lewis Publishers, Boca Raton, 137

Congalton R.G, 1988. A comparison of sampling schemes used in generating error matrices for assessing the accuracy of maps generated from remotely sensed data. Photogrammetric Engineering and Remote Sensing, 54(5), 587-592.

Dupuy, S., et al., 2012. An Object-Based Image Analysis Method for Monitoring Land Conversion by Artificial Sprawl Use of Rapid Eye and IRS Data. Remote Sensing, 4(2), 404-423.

Durieux, L., et al., 2007. A method for monitoring building construction in urban sprawl areas using object-based analysis of Spot 5 images and existing GIS data. ISPRS Journal of Photogrammetry and Remote Sensing, 63, 399-408.

Hay, G.J., Castilla, G., Wulder, M.A., and Ruiz, J.R., 2005. An automated object-based approach for the multiscale image segmentation of forest scenes. International Journal of Applied Earth Observation and Geoinformation, 7(4), 339-359.

Lunetta, R.S., Knight, J.F., Ediriwickrema, J., Lyon, J.G., and Worthy, L.D., 2006. Land-cover change detection using multi-temporal modis ndvi data, Remote Sensing of Environment, 105(2):142-154.

Ma, H.R., Cheng, X., Chen, L., Zhang, H., Xiong, H., 2016. Automatic identification of shallow landslides based on worldview2 remote sensing images, Journal of applied Remote Sensing, 10(1).

Mutangah, J.G., 1994. The vegetation of Lake Nakuru National Park, Kenya; a synopsis of the vegetation types with annotated species list. Journal of East African Natural History, 83, 71-76.

Mwasi, S.M., 2002. Compressed Nature: Co-existing grazers in a small Reserve in Kenya. Doctoral Thesis, Wageningen University.

McFeeters, S.K., 1996. The use of Normalized Difference Water Index (NDWI) in the delineation of open water features, International Journal of Remote Sensing, 17(7):1425-1432.

Oke, A.O.I., Omidiora, E.O., 2012. Effect of Modified Wiener Algorithm on Noise Models, International Journal of Engineering and Technology, 2(8).

Platt, R.V, Rapoza, L., 2008. An evaluation of an Object-oriented paradigm for land use/land covers classification. The Professional Geographer, 60(1), 87-100.

Onywere, S.M., Shisanya, C.A., Obando, J.A., Ndubi, A.O., Masiga, D., Irura, Z., Mariita, N. and Maragia, H.O., 2013. Geospatial extent of 2011-2013 flooding from the East African Rift Valley in Kenya and its implications on the ecosystem. Kenya Soda Lakes Workshop, Kenya Wildlife Service Training Institute, Naivasha, Kenya.

Sakamoto, T., Nguyen, N.V., Kotera, A., Ohno, H., Ishitsuka, N., and Yokozawa, M., 2007. Detecting temporal changes in the extent of annual flooding within the Cambodia and the Vietnamese Mekong Delta from MODIS time-series imagery, Remote Sensing of Environment, 109(3):295–313.

Tiede, D., et al., 2010. Transferability of obia rule sets for idp camp analysis in Darfur. In: The International Archives of the Photogrammetry, Remote Sensing and Spatial Information Sciences, GEOBIA 2010, Geographic Object-Based Image Analysis, Ghent, Belgium.

Tormos, T., et al., 2012. Object-based image analysis for operational fine-scale regional mapping of land covers within river corridors from multispectral imagery and thematic data. International Journal of Remote Sensing, 33(14), pp. 4603-4633.

Tuominen, S., & Pekkarinen, A. (2005). Performance of different spectral and textural aerial photograph features in multi-source forest Inventory. Remote Sensing Environ, 94(2):256-268.